Application of iterative reconstruction algorithms to limited-angle tomography

Seokwon Oh[a], Seungjun Yoo[a], Junho Lee[a], Seongbon Park[a], Taehoon Kim[a], and Ho Kyung Kim [a,*]
[a] *Radiation Imaging Laboratory, School of Mechanical Engineering, Pusan Nat'l Univ., Busandaehakro 63beon-gil, Busan 46241*
[*]*Corresponding author: hokyung@pusan.ac.kr*

***Keywords: Limited-angle tomography, Iterative reconstruction, Out-of-plane ghosting artifact**

1. Introduction

In recent years, the use of lithium-ion batteries and thin-film printed circuit boards (PCBs) has significantly increased with the advancement of electronic devices. For this reason, defect inspection has become more crucial for preventing and mitigating safety accidents. Since these devices are composed of micro-components that are assembled and housed, x-ray inspection is useful for visually revealing the internal structure of the object.

While single projection x-ray imaging allows for fast internal inspection, it has limitations due to the overlapping problem of three-dimensional information onto a two-dimensional plane. This issue poses challenges for defect inspection in multi-layered structured object. To address this problem, a reconstruction of images in three-dimensional space can be employed. However, due to the environmental constraints and efficiency demands of industrial inline inspection, scanning over 180° is impractical [1].

For this reason, a limited-angle tomography (LAT) with less than 180° scan can be considered, but the incomplete scan data causes the depletion in Fourier space. This results in incomplete image reconstruction, which causes out-of-plane ghosting artifacts and distortion, especially for the filtered backprojection (FBP).

Iterative reconstruction (IR), an approach that reconstructs images through iterative projection and backprojection, might alleviate this problem. Each iteration improves the accuracy of the reconstructed image. Although IR algorithms involve high computational complexity due to their iterative nature, they are well known for their ability to produce more accurate and less noisy reconstruction images than FBP. IR algorithms can be divided into various types based on the method used to find the solution. In this study, we applied IR algorithms to LAT and evaluated their performance.

2. Methods and Materials

2.1 Reconstruction algorithms

In this study, FDK [2] and four IR algorithms were applied. The IR algorithms are as follow: simultaneous algebraic reconstruction (SART) [3], least-squares reconstruction with conjugate gradient algorithm (CGLS) [4], SART with total-variation (SART-TV) regularization [5], and statistical reconstruction with the maximum-likelihood expectation-maximization (ML-EM) [6].

The SART iteratively updates the image reconstruction, considering each projection in turn and adjusting the image based on the differences between the measured and estimated projections. However, it may exhibit slower convergence and higher computational demands. The CGLS solves the least-squares problem using conjugate gradients, offering fast convergence and prominent result for sparse system of linear equation. The SART-TV enhances SART by reducing noise and preserving edges through TV regularization. ML-EM iteratively updates the image in a multiplicative way and provides less noisy results.

2.2 Experiment and reconstruction

A linear array of metal beads, an aluminum (Al) disc, and a PCB sample were scanned to assess geometric misalignments and performance. The Al disc and the PCB sample were scanned with a scan angle (α) of 360° and step angle (β) of 1°. The Al disc and the PCB sample were reconstructed for various α, and the β ranges from 1° to 5° for the Al disc and 1° for the PCB sample.

2.3 Evaluation

The performance of the reconstruction algorithms was evaluated based on several metrics. The performance was assessed by comparing the reconstructed images with the reference image, which is FDK image reconstructed with full-scan data.

Out-of-plane ghosting artifacts were analyzed with artifact-spread function (ASF). The ASF is a kind of impulse response function for a thin slice signal along the depth direction (z), and can be measured using the aluminum (Al) disc phantom:

$$\mathrm{ASF}(z) = \frac{\mu_{\mathrm{Al}}(z) - \mu_{\mathrm{bgn}}(z)}{\mu_{\mathrm{Al}}(0) - \mu_{\mathrm{bgn}}(0)}, \quad (1)$$

where $\mu_{Al}(0)$ and $\mu_{bgn}(0)$ are the average pixel values of the Al and neighboring background regions of interest in the reconstructed in-focus ($z = 0$) plane, respectively. $\mu_{Al}(z)$ and $\mu_{bgn}(z)$ represent the respective average pixel values in the off-focus ($z \neq 0$) planes. The CNR and ideal detectability [7] of each algorithm were also evaluated, which were measured at

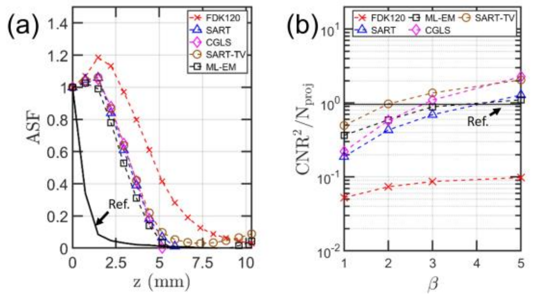

Fig. 1. (a) ASF plots as a function of depth z obtained for various IR algorithms with scan angle of 120° and step angle of 1°. (b) Squared CNR normalized by the number of projections used for reconstruction obtained for various IR algorithms as a function of step angle.

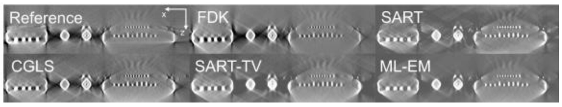

Fig. 2. The sample PCB in-depth images reconstructed using various IR algorithms for the scan angles of 120° and step angle of 1°.

the slice with a thickness of 0.5 mm at $z = 0$ of the Al disc.

3. Preliminary Results

Fig. 1(a) compares the ASF of algorithms at α of 120° and β of 1°. The ASF plot demonstrated ghosting artifacts, or the depth resolution, at the planes out of the in-focus plane. IR showed more improved depth resolution than FDK. ML-EM were somewhat effective for the depth resolution for LAT among IRs.

Fig. 1(b) shows the detectability performance at α of 120°. All IR algorithms dominated the FDK. As the β increased, the detectability of IR algorithms improved, while the FDK almost remained. Moreover, better detectability at smaller is an interesting observation. The SART-TV showed the best for detectability.

Fig. 2 shows the in-depth images of a sample PCB obtained for the α of 120°. The IR algorithms showed less noise and artifacts than FDK; however, the out-of-plane ghosting artifact improvement was not significant.

4. Conclusion

The FBP-based LAT suffers from out-of-plane ghosting artifacts, which enlarges the effective slice thickness. The naive IR methods without incorporation of prior knowledge also showed similar limited depth resolution in LAT. The statistical method adopting an ML-EM algorithm showed the least ghosting artifacts in the reconstructed images. We validated that the IR methods without prior information could not restore missing data in LAT and avoid ghosting artifacts. However, the IR methods are beneficial for better CNR and detectability than the analytical counterpart.

ACKNOWLEDGEMENTS

This work was supported by the National Research Foundation of Korea (NRF) grant funded by the Korea government (MSIT) (No. RS-2024-00340520) and supported by Basic Science Research Program through the National Research Foundation of Korea (NRF) funded by the Ministry of Education (No. RS-2024-00408137).

REFERENCES

[1] N. O'Brien, et al., Recent advances in x-ray cone-beam computed laminography, Journal of X-ray Science and Technology, Vol. 24, No. 5, pp. 691–707, 2016.

[2] L. Feldkamp, et al., Practical cone-beam algorithm, JOASA A, Vol. 1, No. 6, pp. 612-619, 1984

[3] A. Andersen and A. Kak, Simultaneous algebraic reconstruction technique (SART): a superior implementation of the ART algorithm, Ultrasonic imaging, Vol. 6, No. 1, pp. 81-94, 1984.

[4] V. Kulvait and G. Rose, Software implementation of the Krylov methods based reconstruction for the 3D cone beam CT operator, arXiv preprint arXiv:2110.13526, 2021.

[5] X. Luo, et al., An image reconstruction method based on total variation and wavelet tight frame for limited-angle CT, IEEE Access, Vol. 6, pp. 1461-1470, 2017.

[6] K. Lange and R. Carson, EM reconstruction algorithms for emission and transmission tomography, J. Comput. Assist Tomogr., Vol. 8, No. 2, pp. 306-16, 1984.

[7] J. Kim, et al., Towards subtraction angiography using a multi-layered x-ray detector, Physica Medica, Vol. 95, pp. 32-40, 2022.